

## Stereotaxic Device for Optical Imaging of Mice Hind Feet

Richard Cole,<sup>1,2</sup> Timothy Hoffman,<sup>1</sup> Jason Smith,<sup>1</sup> and Bruce Herron<sup>1,2</sup>

<sup>1</sup>Wadsworth Center, New York State Department of Health, Albany, New York 12201, USA; and <sup>2</sup>Department of Biomedical Sciences, School of Public Health, State University of New York at Albany, Albany, New York 12201, USA

Imaging of in vivo model systems, especially mouse models, has revolutionized our understanding of normal and pathological developments. However, mice present several challenges for imaging. They are living and therefore breathing organisms with a fast heart rate (>500 beat/min), which necessitates the need for restraints and positioning controls that do not compromise their normal physiology. We present here a device that immobilizes the rear legs of a mouse while retaining the ability to position both the hind feet and legs for reproducible imaging deep below the skin's surface. The device is highly adjustable to accommodate mice, 5 weeks of age and older. The function of this device is demonstrated by imaging the vasculature ~250  $\mu\text{m}$  beneath the skin in the hind leg. Whereas the overall dimensions are for a motorized stage (Märzhäuser Wetzlar GmbH, Wetzlar, Germany), minor modifications would allow it to be customized for use with most commercially available stages that accept an insert.

**KEY WORDS:** stage insert, multiphoton, angiogenesis, in vivo

### INTRODUCTION

The impetus for developing this device was the need to image changes in the vasculature and vessels (angiogenesis) in response to small molecule modulators. Angiogenesis is the process by which new vessels are created from existing vasculature, in a de novo manner. This process involves interactions among different cell types, in addition to reciprocal interactions of vessels with the surrounding ECM and the hypoperfused tissue. Information can be obtained from simple experimental models, such as cultured endothelial cells; however, cell culture cannot fully demonstrate the complexity of angiogenesis and will always require confirmation of results. Ideally, such confirmatory studies should be carried out by in vivo approaches.<sup>1</sup> To more fully understand angiogenesis, images need to be acquired in three dimensions (3D; ~500  $\mu\text{m}$  deep), thus necessitating the use of multiphoton (MP) imaging. As hair is highly autofluorescent, the hind leg, proximal to the hind paw, is an ideal location to image vasculature, as well as other tissues, as it is devoid of hair follicles. Whereas this device was developed for angiogenesis studies, it is amiable to any study that requires imaging of hairless regions of a mouse, such as blood flow, wound healing, or cell migration.

MP microscopy uses ultrafast, near-infrared laser pulses for the excitation of fluorophores. This excitation is based on nonlinear optical excitation of fluorophores in tissues, such as two or three photon-excited fluorescence. With the use of this technique, excitation occurs only at the focal point of the microscope, thus providing enhanced imaging depth, as well as reduced overall specimen photodamage, photobleaching, and phototoxicity. These advantages make it more suitable for studying intact, living organs/tissues than conventional confocal microscopy. It has become an invaluable optical technique and is used in many disciplines of biology and several different areas of medicine.<sup>2–6</sup>

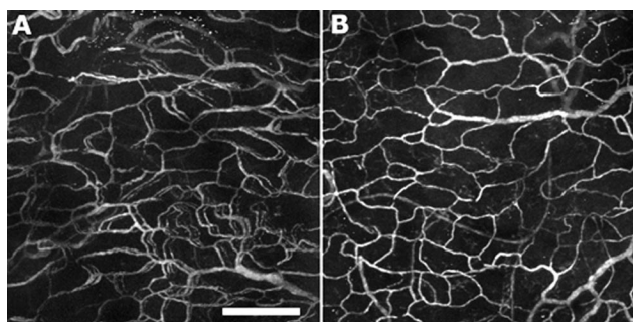
Whereas there is a variety of devices for restraining mice during imaging,<sup>7–13</sup> none was appropriate for restraining a mouse in the proper orientation for imaging of the hind leg. The simplest technique would be to have the mouse on its back and then to tape its toes to a coverslip. However, this technique causes significant blurring and the formation of “double images” of vessels within the 3D volume as a result of movement of the mouse during image acquisition (Fig. 1).

### MATERIALS AND METHODS

#### Animals

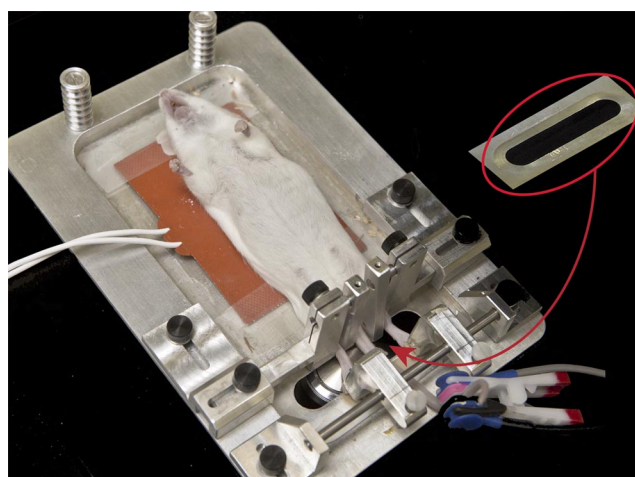
All animals used in this study were handled in accordance with the guidelines of the Wadsworth Center's Institutional Animal Care and Use Committee. A/J and TgN(TIE2GFP)287Sato/J (The Jackson Laboratory, Bar Harbor, ME, USA) mice were used

<sup>1</sup>ADDRESS CORRESPONDENCE TO: Richard Cole, N.Y. State Dept. of Health, Wadsworth Center, P.O. Box 509, Albany, NY 12201, USA (Phone: 518-474-7048; E-mail: rcole@wadsworth.org).  
doi: 10.7171/jbt.13-2403-003


**FIGURE 1**

Maximum intensity projections of dextran-labeled vasculature in 115  $\mu\text{m}$  vol. (A) A mouse imaged while anesthetized but minimally restrained, i.e., mouse on its back toes tapped to coverslip. Note the double image of some vessels and the smearing of other vessels. (B) A mouse imaged while anesthetized and in the stereotaxic device. Note that the vessels appear clear and sharp. Original bar = 40  $\mu\text{m}$ .

in all experiments. Mice were anesthetized by exposure to the inhalation agent isoflurane or through an i.p. injection of 80 mg/Kg ketamine combined with 10 mg/Kg xylazine. Immediately prior to imaging, anesthetized mice were given a 100- $\mu\text{L}$  lateral tail-vein injection of 2% 70 kDa FITC- or TRITC-conjugated dextran (Sigma-Aldrich, St. Louis, MO, USA) in sterile, 200 mM dextrose in 0.9% NaCl. Alternatively, or in combination with the dextran injections, TgN(TIE2GFP)287Sato/J mice were used, which carry a GFP transgene, driven by the endothelial-specific receptor tyrosine kinase (Tie2) promoter, enabling vessel visualization via MP imaging. Mice were then placed on the

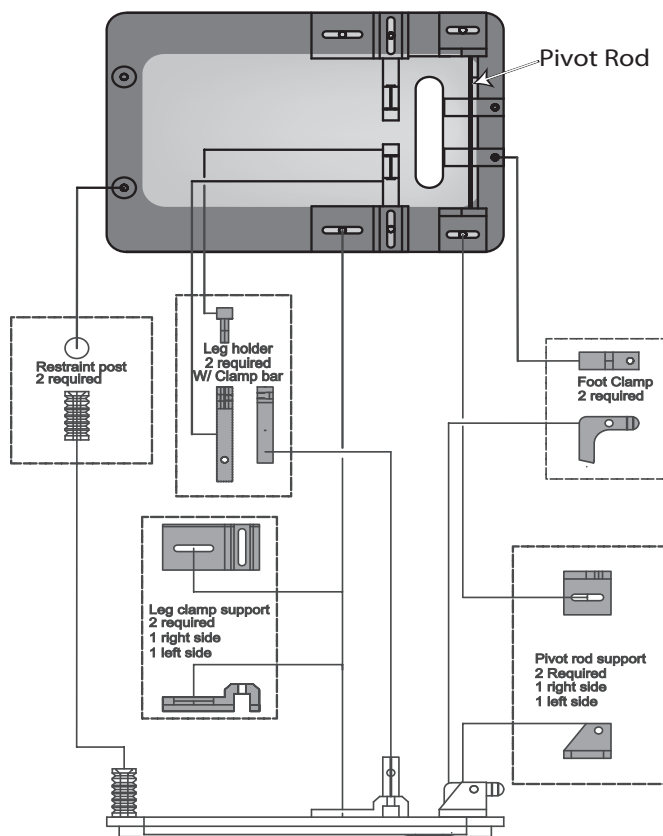

**FIGURE 2**

Photograph of the top view of the device with the anesthetized mouse in place. Note the orange heating pad that is used to maintain the mouse's internal temperature and the MouseOx sensor on the tail of the mouse. The callout (red ellipse) is a bottom view of the imaging area, showing the chamfer machined to allow high NA objective lens clearance and thereby to allow for a larger working area for the objective lens.

stereotaxic device and their hind feet and legs secured (Fig. 2). The rubber-coat foot clamps are adjusted to firmly hold the toes in position. The padding on the toe restraints (Fig. 2; see Machining) assures that the foot is held firmly but without damage to the tissues in the toes. The adjustable leg clamps are used to stabilize the lower leg, further immobilizing the foot region during imaging. For larger mice, their front legs can be secured to the two strait posts via small rubber bands (not shown). Vital signs, including pulse, respiration, and oxygen saturation, were monitored with the MouseOx system (Starr Life Sciences, Oakmont, PA, USA) throughout all procedures.

## Machining

The base of the device was machined from a solid plate, 165  $\times$  115  $\times$  9.5 mm of 6061 aluminum. This metal alloy was chosen for its ease of machine, light weight, as well as its ability to be anodized (corrosion resistance). The restraint systems were also machined from 6061 aluminum blocks of appropriate sizes. The pivot rods were 3.175 mm diameter, 303 stainless steel. As a result of the tight tolerances of reamed holes, ground stainless rods were used to avoid binding or having excessive play in the toe restraints. This alloy and diameter were chosen as a result of their commer-


**FIGURE 3**

Drawing of the stereotaxic device showing all of the salient parts and their location.

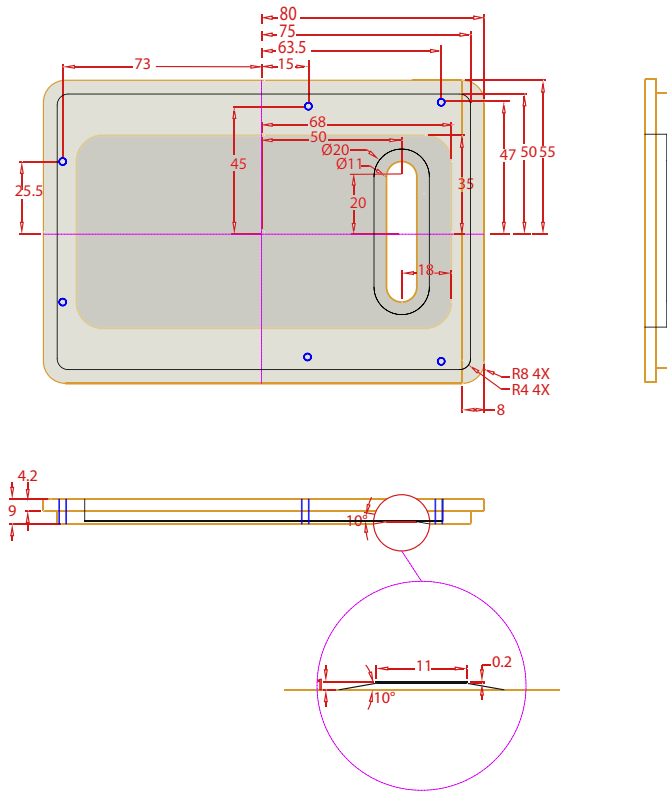


**FIGURE 4**

Mechanical drawing of the stereotactic device, including an enlargement of the objective lens clearance cut. Device is orange, center lines are purple, hidden lines are black, and tapped holes are blue. All dimensions are in millimeters.

cial availability, which reduce machining times. Standard machining practices were used for all parts. A 10° chamfer was cut around the observation slot on the bottom of the tray with an adjustable chamfer end mill (Fleximill 340W; MSC Industrial Supply, Melville, NY). The use of this end mill would allow different chamfer angles to be machined based on the user's objective lens and microscope configuration. Final wall thickness of the observation slot at the opening is 0.2 mm. This was done to facilitate the use of short working distance, i.e., high NA, objectives. Screws are commercially available (303 stainless steel) 4–40 thread, and were equipped with press-on nylon knurled heads to allow for easier adjustment. The ends of foot restraints that come into contact with the toes are dipped into a rubber-coating material (Plasti Dip International, Blaine, NM, USA) before assembly. AutoCAD drawings of all parts are available upon request.

### Imaging

Individual mice were restrained and imaged on a stereotaxic device stage inset (as shown in Fig. 2). The internal temperature of the mouse was maintained by a resistive

heating pad that was held at 37°C. Mice were imaged with a Leica SP5 confocal (Leica, Wetzlar, Germany), equipped for MP imaging (Mai Tai laser; Spectra-Physics, Newport, Irvine, CA, USA). The MP laser was tuned to 760/820 nm to image the FITC/TRITC-labeled dextran and 810 nm to image expressed GFP. Nondescan detectors were used to collect all image data. These detectors are located as close to the objective lens as possible and outside of the confocal scan head, thereby maximizing the signal at the lowest possible photon dose. A 20× (0.7 NA) water objective lens was used to collect all images.

To capture 3D information, Z-stacks (1.2 μm/slice) were collected. Mice anesthetized with ketamine/xylazine had significantly less movement and muscle twitching than did mice anesthetized with isoflurane. Although it is possible to reduce the effects of such movement in the resulting stack projection via 3D digital image processing, less image processing is always more desirable. Isoflurane can be used for the initial anesthesia; however, we recommend that ketamine/xylazine be used as the anesthesia while collecting images.

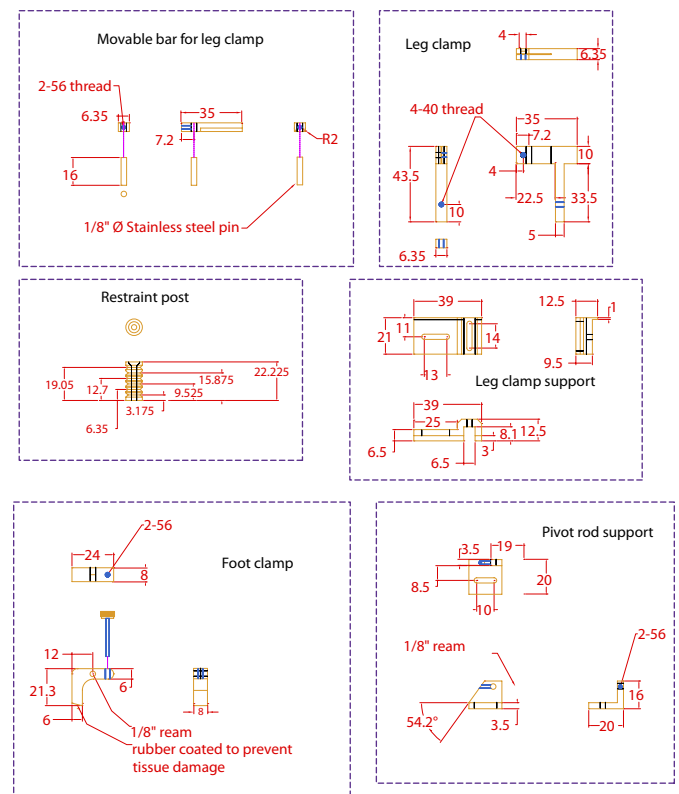


**FIGURE 5**

Mechanical drawing of the restraint apparatus use on the device. Parts are orange, center lines are purple, hidden lines are black, and tapped holes are blue. All dimensions are in millimeters.

## Image Processing

Image stacks were contrast-stretched and histogram-equalized in Fiji.<sup>14</sup> Multichannel stacks were combined, pseudo-colored, and exported as Audio Video Interleave files via Fiji.

## RESULTS AND DISCUSSION

Whereas it is possible to immobilize an animal completely and thereby eliminate all of its movement, the resulting stress and harm to the animal would be unacceptable. The presented stereotaxic device (Figs. 2–5) uses multiple restraint points and has proven to stabilize a mouse's foot mechanically, thereby allowing multichannel 3D imaging, which requires several minutes to complete. We have found no deleterious effect of the device on the mouse's health during imaging or from postimaging examinations. In fact, we used this device routinely during multiple imaging sessions in longitudinal studies spanning 6 weeks with no detectable adverse effects on the mice.<sup>1</sup> Whereas the overall dimensions for the presented device are for a specific motorized stage (Märzhäuser Wetzlar GmbH, Wetzlar, Germany), minor modifications would allow it to be used with most commercially available stages equipped with inserts (Figs. 3–5).

Two-channel, 3D volume through 150  $\mu\text{m}$  depth can be collected routinely (starting s.c. and proceeding anterior) with this method (Supplemental Movie 1). As it is often required that multichannel MP imaging be acquired sequentially, mouse stability is a paramount concern, as any movement within a series or between series will degrade the 3D volume and can cause artifacts, as is clearly visible in Fig. 1. The total collection time for Supplemental Movie 1 was >3 min; this demonstrates further the stability of the mouse's foot held in the device. Whereas it is possible to perform 3D averaging to reduce vessel movement, it inherently causes errors in vessel volume measurements and reduces the accuracy of other measurements.

## ACKNOWLEDGMENTS

This work was supported by the Wadsworth Center Advanced Light Microscopy and Image Analysis Core Facility and grants from the U. S. National Institutes of Health National Institute of Arthritis and Musculoskeletal and Skin Diseases (R01AR054828) and the National Center for Research Resources (1S10RR023451).

## DISCLOSURE

The authors declare no competing interest.

## REFERENCES

1. Cole RW, Lui F, Herron BJ. Imaging of angiogenesis: past, present and future. In Méndez-Vilas A, Díaz J (eds): *Science, Technology, Applications and Education*. Badajoz, Spain: Formatex Research Center, 2010.
2. Brazhe A, Mathiesen C, Lauritzen M. Multiscale vision model highlights spontaneous glial calcium waves recorded by 2-photon imaging in brain tissue. *Neuroimage* 2013;68:192–202.
3. Dancik Y, Favre A, Loy CJ, Zvyagin AV, Roberts MS. Use of multiphoton tomography and fluorescence lifetime imaging to investigate skin pigmentation in vivo. *J Biomed Opt* 2013;18:26022.
4. Hall AM, Rhodes GJ, Sandoval RM, Corridon PR, Molitoris BA. In vivo multiphoton imaging of mitochondrial structure and function during acute kidney injury. *Kidney Int* 2013;83:72–83.
5. Makino T, Jain M, Montrose DC, et al. Multiphoton tomographic imaging: a potential optical biopsy tool for detecting gastrointestinal inflammation and neoplasia. *Cancer Prev Res (Phila)* 2012;5:1280–1290.
6. Zhuo S, Yan J, Chen G, et al. Label-free monitoring of colonic cancer progression using multiphoton microscopy. *Biomed Opt Exp* 2011;2:615–619.
7. Tada T, Wendland M, Watson N, et al. A head holder for magnetic resonance imaging that allows the stereotaxic alignment of spontaneously occurring intracranial mouse tumors. *J Neurosci Methods* 2002;116:1–7.
8. Masihzadeh O, Lei TC, Ammar DA, Kahook MY, Gibson EA. A multiphoton microscope platform for imaging the mouse eye. *Mol Vis* 2012;18:1840–1848.
9. Kamiryo T, Han K, Golfinos J, Nelson PK. A stereotactic device for experimental rat and mouse irradiation using  $\gamma$  knife model B—technical note. *Acta Neurochir (Wien)* 2001;143:83–87.
10. Howles GP, Nouis JC, Qi Y, Johnson GA. Rapid production of specialized animal handling devices using computer-aided design and solid freeform fabrication. *J Magn Reson Imaging* 2009;30:466–471.
11. Davalos D, Lee JK, Smith WB, et al. Stable in vivo imaging of densely populated glia, axons and blood vessels in the mouse spinal cord using two-photon microscopy. *J Neurosci Methods* 2008;169:1–7.
12. Baumann BC, Dorsey JF, Benci JL, Joh DY, Kao GD. Stereotactic intracranial implantation and in vivo bioluminescent imaging of tumor xenografts in a mouse model system of glioblastoma multiforme. *J Vis Exp* 2012;25:pii: 4089.
13. Zinselmeyer BH, Lynch JN, Zhang X, Aoshi T, Miller MJ. Video-rate two-photon imaging of mouse footpad—a promising model for studying leukocyte recruitment dynamics during inflammation. *Inflamm Res* 2008;57:93–96.
14. Schindelin J, Arganda-Carreras I, Frise E, et al. Fiji: an open-source platform for biological-image analysis. *Nat Methods* 2012;9:676–682.